Published in final edited form as:
AJNR Am J Neuroradiol. 2013 May ; 34(5): 958–S1. doi:10.3174/ajnr.A3327.

Improved conspicuity and delineation of high-grade primary and metastatic brain tumors using "restriction spectrum imaging": Quantitative comparison with high b-value DWI and ADC

Nathan S. White, Ph.D.[1], **Carrie R. McDonald, Ph.D.**[2], **Nikdokht Farid, M.D.**[1], **Joshua M. Kuperman, Ph.D.**[1], **Santosh Kesari, M.D.**[3,4,*], and **Anders M. Dale, Ph.D.**[1,3,*]

[1]Department of Radiology, University of California, San Diego, La Jolla, California, USA

[2]Department of Psychiatry, University of California, San Diego, La Jolla, California, USA

[3]Department of Neuroscience, University of California, San Diego, La Jolla, California, USA

[4]Translational Neuro-Oncology Laboratories, Moores Cancer Center, UC San Diego, La Jolla, CA, 92093

Abstract

Background and Purpose—Restriction spectrum imaging (RSI) is a sensitive DWI technique for probing separable water diffusion compartments in tissues. Here, we evaluate RSI tumor cellularity maps (RSI-CM) derived from the spherically-restricted water compartment for improved tumor conspicuity and delineation from non-tumor tissue and reduced sensitivity to edema compared with high b-value DWI and ADC.

Materials and Methods—RSI was performed in 10 pre-surgical patients: 4 with glioblastoma, 3 with primary CNS lymphoma, and 3 with metastatic brain tumors. Multi-directional DWI data was collected at b = 500, 1500, and 4000 sec/mm^2. Quantification of tumor conspicuity (TC), edema conspicuity (EC), and relative sensitivity to edema (RSE) for RSI-CM, DWI at b = 4000 (DWI-4000), and ADC were compared in manually drawn VOIs. Receiver operating characteristic (ROC) curves were used to evaluate the sensitivity and specificity of each method for delineating tumor from NAWM.

Results—Significant TC was seen with both RSI-CM and DWI-4000, but not ADC. Significant EC was seen with ADC, but not RSI-CM or DWI-4000. Significantly greater TC was seen with RSI-CM compared with DWI-4000. Significantly reduced RSE was seen with RSI-CM compared with both DWI-4000 and ADC. Greater sensitivity and specificity for delineating tumor from NAWM was seen with RSI-CM (AUC = .91) compared with both DWI-4000 (AUC = .77) and ADC (AUC = .66).

Address for correspondence: N. S. White, Multimodal Imaging Laboratory, Suite C101; 8950 Villa La Jolla Drive, La Jolla, CA 92037; phone: 858-534-2678; fax: 858-534-1078; nswhite@ucsd.edu.
*Dr. Kesari and Dr. Dale contributed equally to the manuscript as senior authors.

Conflicts of interest: None of the authors have any personal or institutional financial interest in drugs, materials, or devices described in this submission.

Conclusion—RSI-CM offers improved conspicuity and delineation of high-grade primary and metastatic brain tumors and reduced sensitivity to edema compared with high b-value DWI and ADC.

Introduction

DWI is a powerful technique which measures the microscopic diffusion of water at a cellular level [1], and it is routinely utilized for early detection of acute cerebral ischemia [2]. More recently, the clinical utility of DWI has gained increased recognition within neuro-oncology for identifying regions of malignant tumor on the basis of reduced ADC [3–5]. Moreover, numerous investigators have shown a negative correlation between the tumor ADC values and cellularity [6–8], which is commonly attributed to increased *restricted* diffusion imposed by tumor cells. However, despite increased restricted diffusion, tumor ADC values rarely fall below that of normal appearing white matter (NAWM). This is true even in highly cellular tumors that originate in white matter, such as glioblastoma (GBM) and primary CNS lymphoma [9]. One explanation for higher than expected ADC values in these tumors is the presence of vasogenic edema and focal necrosis within the tumor itself, which increase the ADC through reduced *hindrance* imposed on the extracellular water [10, 11]. Thus, increased ADC due to edema and necrosis will offset reduced ADC imposed by tumor cells, resulting in lesions that are difficult to discern from NAWM on the basis of the ADC alone. This effect becomes more pronounced as the b-value is reduced due to increasing sensitivity to the fast, hindered water fraction.

We have recently introduced a DWI technique for multi-b-value, multi-diffusion time acquisitions called “restriction spectrum imaging” (RSI), which aims to separate the hindered and restricted diffusion compartments in tissues over a range, or “spectrum” of length (size) scales with spherical and cylindrical geometries [12]. RSI represents a cross between the high angular resolution diffusion techniques, such as HARDI [13], DSI [14], and Q-Ball [15], and the multi-scale (multi-compartment) methods to probe non-Gaussian diffusion such as bi-exponential [16], stretched exponential [17], and Kurtosis models [18]. As such, RSI requires data be collected over an extended b-value range ($b > 3000$ sec/mm^2) in order to sample non-Gaussian diffusion signal attenuation [19, 20].

The purpose of this study was to evaluate the clinical utility of the RSI method for improved delineation of tumor from NAWM as well as reduced sensitivity to edema and necrosis compared to DWI and ADC image contrast measured at equivalent high b-values. We hypothesize that by isolating signal from the spherically-restricted water fraction with RSI, one may achieve greater sensitivity and specificity to tumor cellularity in the presence of edema and necrosis, which may allow for improved delineation of tumor from NAWM compared with DWI and ADC.

Methods

Patients

This prospective study was approved by our institutional review board and written informed consent was obtained from all patients. Between 2010 and 2012, all of the patients seen at

the Neuro-Oncology department at the University of California, San Diego, Moores Cancer Center underwent a standardized MRI protocol which included the RSI sequence. To limit the potential confound of surgical effects, patients were only included in this study if they had received an RSI scan *prior* to surgical resection. This resulted in a total of 10 patients that included 4 GBMs, 3 primary CNS lymphomas, and 3 metastatic tumors (Table 1). All patients with primary brain tumors were histologically diagnosed based on either pre-imaging biopsy or post-imaging biopsy or resection. Patients with metastatic tumors had known primary malignancies.

MR Imaging Examination

MR imaging was performed on a 3.0T GE Signa Excite HDx scanner equipped with a 8-channel head coil. Our imaging protocol included pre- and post-Gadolinium 3D volumetric T1-weighted IR-SPGR sequences (TE/TR = 2.8/6.5ms; TI = 450ms; FA = 8°; FOV = 24cm; 0.93×0.93×1.2mm) and a 3D T2-weighted FLAIR sequence (TE/TR = 126/6000ms; TI = 1863ms; FOV = 24cm; 0.93×.093×1.2mm). For RSI, a single-shot pulsed-field gradient spin-echo (PGSE) echo-planar imaging (EPI) sequence was used (TE/TR = 96ms/17s; FOV = 24cm, matrix = 96×96×48) with 4 b-values (b = 0, 500, 1500, and 4000 s/mm^2), and 6, 6, and 15 unique diffusion directions for each non-zero b-value, respectively (28 total volumes, ~8 min scan time).

Preprocessing, ADC and DWI Calculation

Prior to analysis, the raw RSI data were corrected for geometric distortions due to susceptibility [21], gradient nonlinearities, and eddy currents. This was followed by correction of patient motion using in-house software. The ADC was calculated from a tensor fit to the full dataset (all b-values and diffusion directions). DWI images were formed separately for each b-value by averaging the b = 500 (DWI-500), b = 1500 (DWI-1500), and b = 4000 (DWI-4000) data.

RSI Analysis

For fixed diffusion time acquisitions, the RSI model reduces to a spectrum of ADC's at each voxel of the form [12]:

$$S = S_0[\sum_i \exp(-bADC_i)]; ADC_i = \left(ADC_{\parallel} - ADC_{\perp}^{(i)}\right)\cos^2\alpha + ADC_{\perp}^{(i)} \quad [1]$$

where $ADC_{\parallel}$ and $ADC_{\perp}$ are the apparent parallel and perpendicular diffusivities of a cylindrical tissue element, α is the angle between the cylinder (long) axis and the diffusion gradient direction, and S0 is the signal measured at b = 0. To define the spectrum, we set $ADC_{\parallel} = 1 \times 10^{-3}$ mm2/sec and vary $ADC_{\perp}$ from 0 mm^2/sec to $ADC_{\parallel}$ in six equally spaced steps (Supplementary Fig. 1A, Scales 1–6). Two additional isotropic terms were included, one modeling restricted diffusion ($ADC_{\parallel} = ADC_{\perp} = 0$ mm^2/sec, Supplementary Fig 1A, Scale 0) and one "free" water ($ADC_{\parallel} = ADC_{\perp} = 3 \times 10^{-3}$ mm^2/sec, Supplementary Fig 1B, Scale 7). To account for the unknown orientation of the cylindrical components (Scales 1–6, where $ADC_{\perp} < ADC_{\parallel}$), we used a spherical harmonic (SH) expansion for their orientation distribution functions as detailed in [12] (not shown in Eq [1] for simplicity). Parameter

maps were then fit to the unnormalized signal, which included the ADC spectrum components (T2-weighted volume fractions, Supplementary Fig 1B) and the geometric components (SH coefficients, not shown), using least-squares estimation with Tikhonov regularization [12]. A constrained minimum variance beamformer was used to combine all the parameter maps (diffusion spectra) post hoc into a single image (herein termed the "RSI cellularity map", or RSI-CM Supplementary Fig 1E) with maximum specificity to spherical restricted diffusion (Scale 0) through attenuation of signal from all other scales (Scales 1–7).

Volumes-of-Interest (VOIs)

Manual VOIs were drawn for tumor, peritumoral edema, and NAWM using co-registered 3D volumetric T1 post-contrast, 3D volumetric FLAIR, and ADC sequences by a board certified neuroradiologist using the Amira® software package (Visage Imaging, Inc.). Tumor was identified as areas of low ADC within the primary enhancing tumor site identified on the T1 post-contrast sequence. Peritumoral edema was identified as regions of hyperintensity on FLAIR surrounding the primary tumor. NAWM was drawn in white matter contralateral to the tumor.

Conspicuity and Relative Sensitivity to Edema

To objectively quantify tumor conspicuity (TC) and edema conspicuity (EC) on imaging, we computed intensity ratios for each patient by dividing the mean signal in tumor and edema, respectively, by the mean signal in NAWM (TC = Tumor/NAWM; EC = Edema/NAWM). To quantify the relative sensitivity to edema (RSE) versus sensitivity to tumor we again computed intensity ratios—dividing the mean signal in edema by the mean signal in tumor (RSE = Edema/Tumor). RSE values greater than 1 indicate greater relative sensitivity to edema versus tumor, and RSE values less than 1 indicate greater relative sensitivity to tumor versus edema. It should be noted that the RSE as a measure is not reliant on the assumption that the peritumoral edema is not infiltrated (as one would expect for GBM), only that the relative proportion of tumor cells be greater in our tumor VOI compared with our edema VOI. As an exploratory analysis, we also calculated a *predicted infiltration baseline (PIB)*, defined here as the fractional difference between the mean signal in NAWM and the mean signal in edema divided by the mean signal in tumor (PIB = 100*[NAWM – Edema]/Tumor for RSI-CM and DWI, and 100*[Edema - NAWM]/Tumor for ADC). The PIB was deemed significant because it provides a theoretical measure of the minimal amount of tumor infiltration (signal) that would be needed within edema for it to be distinguished from NAWM. Note, for ADC, a sign change is applied to the PIB to reflect the contrast reversal between tumor and edema. Also note, a negative PIB as defined above would suggest infiltrating tumor.

ROC analysis

To quantify the overall sensitivity and specificity of each method in distinguishing tumor from NAWM, we computed ROC curves by plotting the cumulative distribution of the normalized tumor signal intensity histograms compiled across all patients (sensitivity), against the normalized NAWM signal intensity histograms compiled across all patients (1-specificity).

Results

Qualitative improvements in tumor conspicuity and visualization of tumor margins were observed in all patients with RSI-CM compared to DWI-4000 and ADC. Three representative patients are shown in Figs 1–3 for glioblastoma, lymphoma, and metastatic disease, respectively.

Quantitative comparisons of TC, RSE, and PIB are shown in Fig 4 and Table 2. Significant TC was noted on RSI-CM [$t(9) = 4.67$, $p = .001$] and DWI-4000 [$t(9) = 3.68$, $p = .005$], but not on ADC [$t(9) = -1.75$, $p = .11$]. Furthermore, RSI-CM demonstrated significantly greater TC compared with DWI-4000 [$t(9) = 4.48$, $p = .002$] and ADC [$t(9) = 6.73$, $p < .001$]. Significant EC was noted on ADC [$t(9) = 5.76$, $p < .001$], but not on RSI-CM [$t(9) = 1.02$, $p = .34$] or DWI-4000 [$t(9) = 1.78$, $p = .11$]. Significantly reduced RSE was noted for RSI-CM compared with DWI-4000 [$t(9) = -11.69$, $p < .001$] and ADC [$t(9) = -17.83$, $p < .001$]. ADC demonstrated significantly greater **PIB** compared with RSI-CM [$t(9) = 3.34$, $p < .01$] and DWI-4000 [$t(9) = 3.99$, $p < .01$].

ROC curves are presented in Fig 6, showing the greater sensitivity and specificity for distinguishing tumor from NAWM with RSI-CM (AUC = .91) compared with both DWI-4000 (AUC = .77) and ADC (AUC = .66).

Discussion

Restriction spectrum imaging (RSI) is a sensitive DWI technique that allows for probing separable hindered and restricted water compartments in tissues across a spectrum of length scales and geometries. Here, we evaluate the utility of RSI cellularity maps (RSI-CM) in a clinical setting to improve tumor conspicuity and delineation from NAWM compared with high b-value DWI and ADC.

Early detection of brain tumors on MRI requires images with high contrast between tumor and non-tumor tissue. In all patients, we noted qualitative improvements in tumor conspicuity with RSI-CM compared with both high b-value DWI and ADC. These findings were supported by quantitative analyses demonstrating significantly improved tumor conspicuity on RSI-CM compared with DWI-4000 and ADC (Fig 4A). Conspicuity on ADC was only significant for edema, but not tumor (Fig 4A). Partial voluming of edema and necrosis within the tumor may contribute to reduced conspicuity of tumor on ADC, and conversely removal of the fast hindered water component due to intra-tumoral edema and necrosis may explain in part the enhanced conspicuity of tumor on RSI-CM.

Imaging sequences that are highly sensitive in detecting treatment-related changes in tumor versus edema are critical in the longitudinal evaluation of brain tumors, especially when the treatment is known to significantly alter the level of vasogenic edema, as seen with agents that inhibit the vascular endothelial growth factor pathways (anti VEGF agents) [22]. The results in Fig 4B demonstrate significantly reduced relative sensitivity to edema versus tumor (RSE) with RSI-CM compared to DWI-4000 and ADC. The significantly higher RSE on ADC implies reduced ability to assess treatment-related changes in tumor cellularity in

the setting of concurrent changes in edema, compared with RSI-CM and DWI-4000 (Fig 4B).

Detecting the extent of infiltrating tumor within peritumoral edema also requires high sensitivity to tumor relative to edema, which corresponds to low RSE. Many authors have examined the role of the ADC to differentiate tumor-infiltrated edema from purely vasogenic edema, but the consensus remains mixed. While some have found higher ADC values in the presumably infiltrated peritumoral edema of high-grade gliomas compared with meningiomas [23, 24], others have found the opposite relation (higher ADC values in the peritumoral edema of menigiomas compared with high-grade gliomas) [4, 25–27]. Such conflicting results are consistent with the high sensitivity of the ADC to variations in the level of edema. While the current study was not designed to systematically test the ability of RSI-CM to differentiate infiltrated edema from purely vasogenic edema, we did note significant improvements in the predicted infiltration baseline (PIB) with RSI-CM and DWI-4000 compared with ADC (Fig 4C). This measure simply reflects the percentage of tumor signal that is required to reduce (in the case of ADC) or increase (in the case of RSI-CM and DWI-4000) the existing edema signal to that of NAWM. Only the ADC demonstrated significantly elevated PIB (Fig 4C), suggesting reduced ability to distinguish infiltrating tumor in peritumoral regions. Consistent with the theoretical prediction of the PIB, we did note qualitative differences in the GBM tumor margins compared with the metastatic (presumably non-infiltrating) tumor margins on RSI-CM compared with the ADC, an example of which is demonstrated in Fig 5. However, to systematically test whether or not RSI-CM may provide a more reliable biomarker of tumor infiltration compared to the ADC will require further validation on a larger sample size in conjunction with histological evidence of infiltration.

Consistent with the increased tumor conspicuity and reduced relative sensitivity to edema, we observed greater sensitivity and specificity for delineating tumor from NAWM with RSI-CM compared with DWI-4000 and ADC (Fig 6). We also observed greater heterogeneity of tumor signal intensities (as evidenced by a broader histogram distribution) on RSI-CM compared with DWI-4000 and ADC (Fig 6), which may reflect the intrinsic heterogeneity of tumor cellularity both within and across tumor types. If so, RSI-CM may provide an improved tool for directing biopsies to the most cellular aspects of patient’s tumor, which may improve diagnosis and treatment planning.

There are a number of limitations to our study. First, only a small number of patients were selected due to the stringent criteria of including only pre-surgical tumors, and of those selected patients some received radiation therapy prior to imaging and some did not. The purpose of the pre-surgical criteria was to mitigate any confound of post-surgical resection on our imaging comparisons, such as cytotoxic edema, blood products, etc. While incorporating patients with and without radiation therapy is not an ideal study design, we would not expect any systematic bias for one image contrast over another for two reasons. First, although radiation treatment is known to cause vasogeneic edema and focal necrosis in tumor and surrounding tissue, it also reduces tumor cellularity and therefore such treatment will result in reduced contrast between tumor and NAWM in both RSI-CM and ADC. Second, our tumor VOIs incorporated only the portion of contrast enhancing viable tumor

that demonstrated reduced ADC, which would exclude tissue with significant radiation necrosis and edema from the analyses. Finally, while our study demonstrates improved tumor contrast and reduced sensitivity to edema on RSI-CM compared to high b-value DWI and ADC, our analyses were based on averaging signal characteristic across high-grade primary and metastatic tumors. Further study is needed to systematically evaluate RSI cellularity biomarkers across tumor-types in addition to post-operative histopathological validation of cellularity signals.

Conclusion

RSI cellularity maps offer improved conspicuity and delineation of high-grade primary and metastatic brain tumors and reduced sensitivity to edema compared with high b-value DWI and ADC, which may facilitate earlier detection of residual, recurrent, and infiltrating brain tumors.

Supplementary Material

Refer to Web version on PubMed Central for supplementary material.

Acknowledgments

Funding: grants R01AG031224, R01EB000790 (N.S.W), RC2 DA29475 (A.M.D.), EB00790-06 (A.M.D.) and 3P30CA023100-25S8 (S.K.)

We would like to thank patients and staff at UC San Diego Neuro-Oncology Program for their generous participation.

Abbreviation key

RSI	Restriction spectrum imaging
RSI-CM	RSI cellularity map
TC	Tumor Conspicuity
EC	Edema Conspicuity
RSE	Relative sensitivity to edema
NAWM	Normal appearing white matter
PIB	Predictive Infiltration Baseline
ROC	Receiver operating characteristic
AUC	ROC Area Under The Curve

References

1. Le Bihan D. Molecular diffusion nuclear magnetic resonance imaging. Magn Reson Q. 1991; 7(1): 1–30. [PubMed: 2043461]
2. Lutsep HL, Albers GW, DeCrespigny A, Kamat GN, Marks MP, Moseley ME. Clinical utility of diffusion-weighted magnetic resonance imaging in the assessment of ischemic stroke. Ann Neurol. 1997; 41(5):574–580. [PubMed: 9153518]

3. Kono K, Inoue Y, Nakayama K, et al. The role of diffusion-weighted imaging in patients with brain tumors. AJNR Am J Neuroradiol. 2001; 22(6):1081–1088. [PubMed: 11415902]
4. Krabbe K, Gideon P, Wagn P, Hansen U, Thomsen C, Madsen F. MR diffusion imaging of human intracranial tumours. Neuroradiology. 1997; 39(7):483–489. [PubMed: 9258924]
5. Sundgren PC, Fan X, Weybright P, et al. Differentiation of recurrent brain tumor versus radiation injury using diffusion tensor imaging in patients with new contrast-enhancing lesions. Magn Reson Imaging. 2006; 24(9):1131–1142. [PubMed: 17071335]
6. Sugahara T, Korogi Y, Kochi M, et al. Usefulness of diffusion-weighted MRI with echo-planar technique in the evaluation of cellularity in gliomas. J Magn Reson Imaging. 1999; 9(1):53–60. [PubMed: 10030650]
7. Chen J, Xia J, Zhou YC, et al. Correlation between magnetic resonance diffusion weighted imaging and cell density in astrocytoma. Zhonghua Zhong Liu Za Zhi. 2005; 27(5):309–311. [PubMed: 15996330]
8. Guo AC, Cummings TJ, Dash RC, Provenzale JM. Lymphomas and high-grade astrocytomas: comparison of water diffusibility and histologic characteristics. Radiology. 2002; 224(1):177–183. [PubMed: 12091680]
9. Maier SE, Sun Y, Mulkern RV. Diffusion imaging of brain tumors. NMR Biomed. 2010; 23(7): 849–864. [PubMed: 20886568]
10. Chenevert TL, Sundgren PC, Ross BD. Diffusion imaging: insight to cell status and cytoarchitecture. Neuroimaging Clin N Am. 2006; 16(4):619–632. viii–ix. [PubMed: 17148023]
11. Nicholson C. Factors governing diffusing molecular signals in brain extracellular space. J Neural Transm. 2005; 112(1):29–44. [PubMed: 15372328]
12. White N, Leergaard T, D'Arceuil H, Bjaalie J, Dale A. Probing tissue microstructure with restriction spectrum imaging: histological and theoretical validation. Human Brain Mapping. In Press.
13. Frank LR. Characterization of anisotropy in high angular resolution diffusion- weighted MRI. Magn Reson Med. 2002; 47(6):1083–1099. [PubMed: 12111955]
14. Wedeen VJ, Hagmann P, Tseng WY, Reese TG, Weisskoff RM. Mapping complex tissue architecture with diffusion spectrum magnetic resonance imaging. Magn Reson Med. 2005; 54(6): 1377–1386. [PubMed: 16247738]
15. Tuch DS. Q-ball imaging. Magn Reson Med. 2004; 52(6):1358–1372. [PubMed: 15562495]
16. Maier SE, Bogner P, Bajzik G, et al. Normal brain and brain tumor: multicomponent apparent diffusion coefficient line scan imaging. Radiology. 2001; 219(3):842–849. [PubMed: 11376280]
17. Bennett KM, Schmainda KM, Bennett RT, Rowe DB, Lu H, Hyde JS. Characterization of continuously distributed cortical water diffusion rates with a stretched-exponential model. Magn Reson Med. 2003; 50(4):727–734. [PubMed: 14523958]
18. Jensen JH, Helpern JA, Ramani A, Lu H, Kaczynski K. Diffusional kurtosis imaging: the quantification of non-gaussian water diffusion by means of magnetic resonance imaging. Magn Reson Med. 2005; 53(6):1432–1440. [PubMed: 15906300]
19. Mulkern RV, Haker SJ, Maier SE. On high b diffusion imaging in the human brain: ruminations and experimental insights. Magn Reson Imaging. 2009; 27(8):1151–1162. [PubMed: 19520535]
20. Mulkern RV, Gudbjartsson H, Westin CF, et al. Multi-component apparent diffusion coefficients in human brain. NMR Biomed. 1999; 12(1):51–62. [PubMed: 10195330]
21. Holland D, Kuperman JM, Dale AM. Efficient correction of inhomogeneous static magnetic field-induced distortion in Echo Planar Imaging. Neuroimage. 2010; 50(1):175–183. [PubMed: 19944768]
22. Gerstner ER, Chen PJ, Wen PY, Jain RK, Batchelor TT, Sorensen G. Infiltrative patterns of glioblastoma spread detected via diffusion MRI after treatment with cediranib. Neuro Oncol. 2010; 12(5):466–472. [PubMed: 20406897]
23. Provenzale JM, McGraw P, Mhatre P, Guo AC, Delong D. Peritumoral brain regions in gliomas and meningiomas: investigation with isotropic diffusion-weighted MR imaging and diffusion-tensor MR imaging. Radiology. 2004; 232(2):451–460. [PubMed: 15215555]
24. Bastin ME, Sinha S, Whittle IR, Wardlaw JM. Measurements of water diffusion and T1 values in peritumoural oedematous brain. Neuroreport. 2002; 13(10):1335–1340. [PubMed: 12151798]

25. Chiang IC, Kuo YT, Lu CY, et al. Distinction between high-grade gliomas and solitary metastases using peritumoral 3-T magnetic resonance spectroscopy, diffusion, and perfusion imagings. Neuroradiology. 2004; 46(8):619–627. [PubMed: 15243726]

26. Lu S, Ahn D, Johnson G, Cha S. Peritumoral diffusion tensor imaging of high-grade gliomas and metastatic brain tumors. AJNR Am J Neuroradiol. 2003; 24(5):937–941. [PubMed: 12748097]

27. Tsuchiya K, Fujikawa A, Nakajima M, Honya K. Differentiation between solitary brain metastasis and high-grade glioma by diffusion tensor imaging. Br J Radiol. 2005; 78(930):533–537. [PubMed: 15900059]

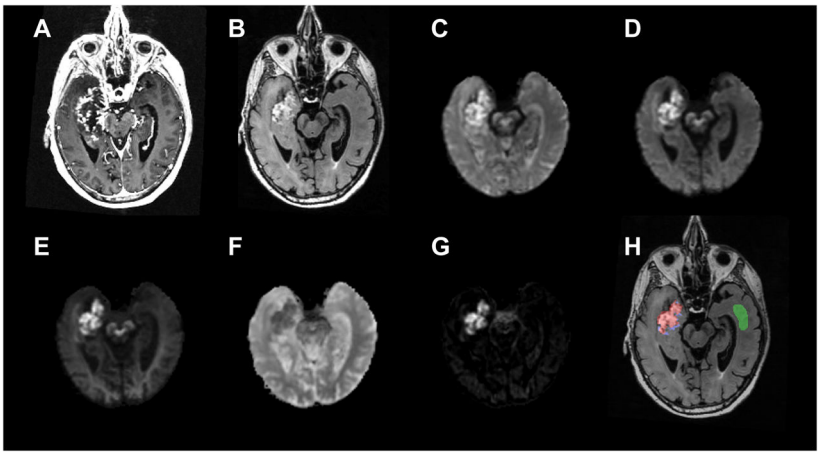

Figure 1.

Anatomic T1-weighted post contrast (A) and T2-weighted FLAIR (B) for a 84/M with glioblastoma (patient #3). Shown also are DWI images at b=500 (C), b=1500 (D), and b=4000 (E), ADC (F), and RSI-CM (G). VOIs for tumor (red), peritumoral edema (blue), and NAWM (green) used for quantitative analysis are shown in (H).

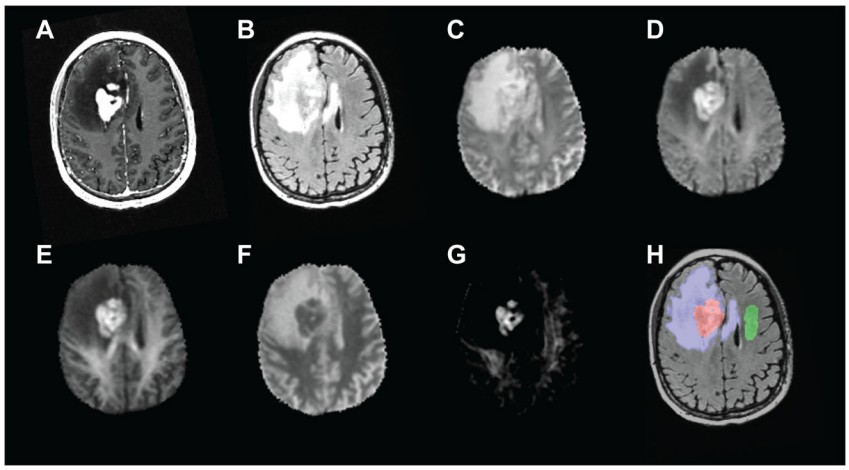

Figure 2.

Anatomic T1-weighted post contrast (A) and T2-weighted FLAIR (B) for a 67/M with lymphoma (patient #7). Shown also are DWI images at b=500 (C), b=1500 (D), and b=4000 (E), ADC (F), and RSI-CM (G). VOIs for tumor (red), peritumoral edema (blue), and NAWM (green) used for quantitative analysis are shown in (H).

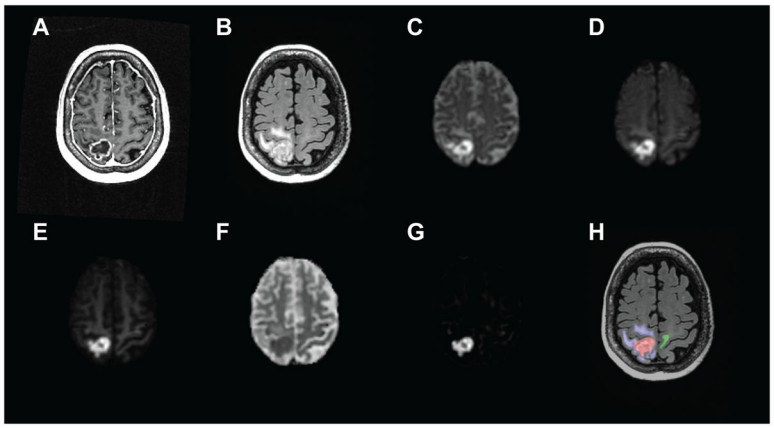

Figure 3.

Anatomic T1-weighted post contrast (A) and T2-weighted FLAIR (B) for a 73/F with metastatic non-small cell lung cancer (patient #10). Shown also are DWI images at b=500 (C), b=1500 (D), and b=4000 (E), ADC (F), and RSI-CM (G). VOIs for tumor (red), peritumoral edema (blue), and NAWM (green) used for quantitative analysis are shown in (H).

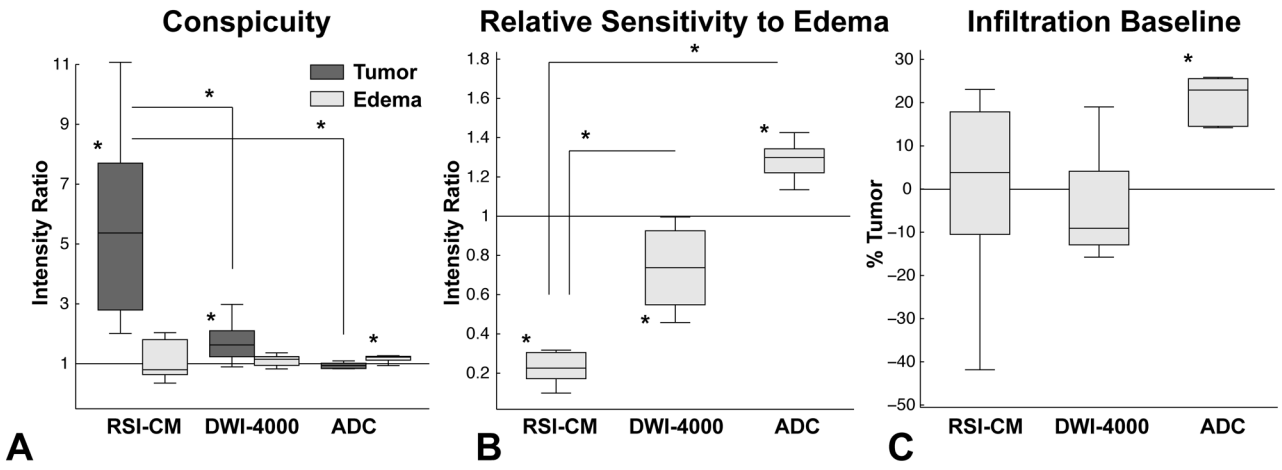

Figure 4.

Box-and-whisker plots of intensity ratios quantifying tumor and edema conspicuity (A) and relative sensitivity to edema (B). On each box, the central mark is the median, the edges of the box are the 25th and 75th percentiles, the whiskers represent data ranges, and the red dots indicate potential outliers. A, TC was significant on RSI-CM ($p = .001$) and DWI-4000 ($p = .005$), but not ADC ($p = 0.11$). TC was significantly greater on RSI-CM compared with DWI-4000 ($p = .002$) and ADC ($p < .001$). B, RSE was significantly less in RSI-CM versus DWI-4000 ($p < .001$) and ADC ($p < .001$). (C) Box-and-whisker plots of the infiltrative baseline, defined as the percentage of tumor signal required within edema to equalize the signal to NAWM. The infiltrative baseline of ADC was significantly greater than RSI-CM ($p < .001$) and DWI-4000 ($p < .001$). Note: negative datapoints may reflect tumor infiltrated edema. TC – Tumor Conspicutiy, EC –Edema Conspicuity, RSE – Relative sensitivity to edema.

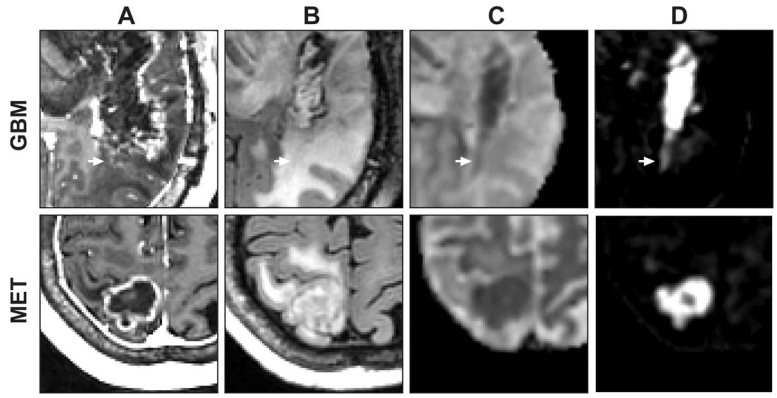

Figure 5.

Close-up comparison of GBM (patient # 2) and non small cell lung metastasis (patient # 10). Anatomic T1-weighted post contrast (A), T2-weighted FLAIR (B), (C) ADC, and (D) RSI-CM. Arrows indicates region of possible GBM tumor infiltration in non-enhancing peritumoral edema.

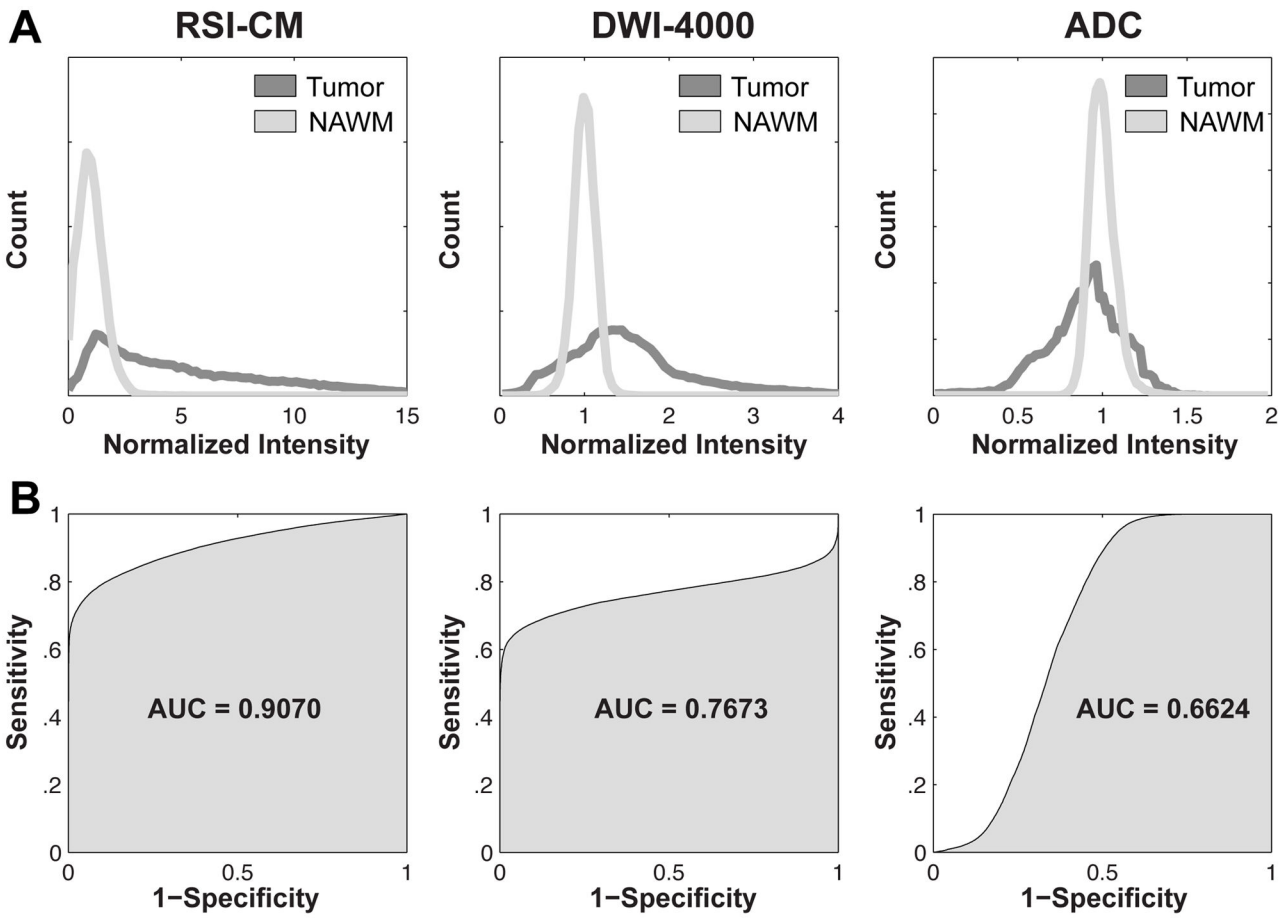

Figure 6.

Shown are normalized intensity histograms (A) and corresponding ROC curves (B) quantifying the increased sensitivity and specificity and overall accuracy (AUC) of RSI-CM for distinguishing tumor from NAWM compared with DWI-4000, and ADC.

Table 1

Histological diagnosis and patient demographics.

Patient	Gender	Age	Pathology	Status
#1	Male	51	Glioblastoma, astrocytic, gemistocytic	Post-biopsy Post-radiation (6 months)*
#2	Male	53	Glioblastoma, astrocytic, small cell	Post-biopsy Post-radiation (8 months)*
#3	Male	84	Glioblastoma, astrocytic, small cell	Pre-biopsy Pre-radiation
#4	Male	66	Glioblastoma, astrocytic, gemistocytic	Pre-biopsy Pre-radiation
#5	Male	55	Primary CNS Lymphoma, Large B-cell	Post-biopsy Pre-radiation
#6	Female	74	Primary CNS Lymphoma, Large B-cell	Pre-biopsy Pre-radiation
#7	Male	67	Primary CNS Lymphoma, Large B-cell	Pre-biopsy Pre-radiation
#8	Female	72	metastastic adenocarcinoma, primary colon	Pre-biopsy Post-radiosurgery (14 months)*
#9	Male	58	metastatic renal cell carcinoma	Pre-biopsy Post-radiosurgery (10 months)*
#10	Female	73	Metastatic non-small cell lung	Pre-biopsy, Post-radiosurgery (6 months)*

* Interval in months between radiation treatment and MRI scan

Table 2

Quantitative image contrast measures.

	RSI-CM	DWI-4000	ADC
Tumor Conspicuity (TC) (A/C)	5.78 (3.23)	1.71 (0.61)	0.91 (0.16)
Edema Conspicuity (EC) (B/C)	1.50 (1.57)	1.17 (0.31)	1.19 (0.10)
Relative Sensitivity to Edema (RSE)* (B/A)	0.24 (0.12)	0.73 (0.20)	1.33 (0.17)
Predicted Infiltration Baseline (%)** (C-B)/A *100 for RSI-CM, DWI-4000 -(C-B)/A *100 for ADC	0.01 (19.68)	−7.57 (17.78)	18.69 (11.34)

Note: A = **Mean intensity in Tumor**, B = **Mean intensity in Edema**, C = **Mean intensity in NAWM**.

*Values less than 1 indicate greater relative sensitivity to tumor versus edema and values greater than 1 indicate greater relative sensitivity to edema versus tumor.

**negative values may reflect tumor infiltrated edema.